American Mineralogist, Volume 63, pages 898–912, 1978

Regional metamorphism of Proterozoic iron-formation, Labrador Trough, Canada

CORNELIS KLEIN

Department of Geology, Indiana University
Bloomington, Indiana 47401

Abstract

The Proterozoic iron-formation in the south-central part of the Labrador Trough is the product of primary sedimentation and of diagenesis, but south of the Grenville Front this same iron-formation exhibits the effects of metamorphic conditions that range from greenschist through amphibolite to granulite facies. Although the iron-formation is not continuous where the Labrador Trough sequences have become involved in the Grenville Orogeny, sampling and study of discontinuous iron-formation assemblages allows an overview of the changes in assemblages and chemical composition of coexisting minerals in prograde metamorphosed iron-rich sediments. Late diagenetic assemblages are rich in chert, carbonates (siderite, dolomite to ankerite, calcite), magnetite, hematite, greenalite, stilpnomelane, and minnesotaite. Amphibolite facies iron-formation contains abundant Fe–Mg clinoamphiboles and Ca-clinoamphiboles, as well as iron oxides and Fe-rich carbonates. The highest metamorphic grade iron-formation assemblages are rich in orthopyroxene, with lesser clinopyroxene. Specific assemblages and compositional ranges for minerals in the iron-formations and closely associated rock types are listed and shown graphically. Although there is a general trend toward dehydration and decarbonation with increasing metamorphic grade, local assemblage inconsistencies illustrate that CO_2 and H_2O have generally not behaved as perfectly mobile components. The activity of O_2 has been rather narrowly buffered by magnetite–hematite coexistences from diagenetic through high-grade metamorphic conditions. The range of physical conditions represented by the assemblages is from about 150°C at 1–2 kbar to about 700–750°C at 10–11 kbar.

Introduction

The extensive Proterozoic iron-formations in the central and southern Labrador Trough afford an excellent opportunity to study the changes in mineral assemblages as a function of changing metamorphic grade. Gross (1968) showed that the iron-formations which occur in the western part of the Labrador Trough can be traced for about 700 miles. In the southern part of the Labrador Trough the unmetamorphosed iron-formation passes into the Grenville orogenic belt and becomes highly folded, faulted, and metamorphosed. Fahrig (1967) shows the biotite isograd crossing the Labrador Trough approximately 12 miles south of Sawbill Lake (Fig. 1). This isograd probably is the northernmost expression of the Grenville orogenic belt (Grenville Front).

The chemistry, mineralogy, and assemblages of the unmetamorphosed iron-formations in the central Labrador Trough have been studied recently by Klein (1974), Klein and Fink (1976), Klein and Bricker (1977), Lesher (1976), and Zajac (1974). Petrologic studies of metamorphic iron-formation assemblages in the area south of the biotite isograd (Fig. 1) have been made by Mueller (1960) in the Bloom Lake area, by Kranck (1961) in the Mount Reed and Hobdad Lake areas, by Klein (1966) in the Labrador City area, and by Butler (1969) in the Gagnon–Mount Reed–Lac des Silicates area (for locations see Fig. 1). Each of these four studies was restricted to iron-formation assemblages of a specific and restricted metamorphic grade. This study provides an *overview* of the assemblages in iron-formation and the mineralogic changes therein as a function of regionally increasing metamorphic grade. The often-made assumption that iron-formations are rather simple chemical systems is not supported by the observed complexity of assemblages. The lowest-grade assemblages, from the Howells River area (Klein, 1974; Klein and Fink, 1976), represent late-diagenetic (essentially unmetamorphosed) condi-

0003-004X/78/0910-0898$02.00

tions, whereas those of the Gagnon region were metamorphosed in upper amphibolite to granulite conditions.

Handspecimen and diamond drill core samples of iron-formation, and, wherever possible, of closely associated rock types, were obtained from the various localities listed in Figure 1. In the original field selection of samples I concentrated on the most highly varied and complex assemblages. Although banded qtz[1] (or chert)–mag, qtz–hem, or qtz–hem–mag assemblages are present in many of the localities listed in Figure 1, and constitute the ore zones in the mining areas, such assemblages provide no insight into metamorphic reactions among carbonates, oxides, or silicates. Of the field and diamond drill core samples approximately 270 were studied by optical microscope (transmitted and reflected light), and for 137 of these each mineral in the assemblage was analyzed quantitatively for nine oxide components by electron microprobe techniques. On complex assemblages, between 30 to 40 nine-element probe analyses were made, on an average, and on the most simple assemblages about ten. The total number of such analyses used in this study is approximately 2400. The electron microprobe procedure is outlined in Klein (1974).

Bulk chemistry of the iron-formations

Twenty-three representative samples of iron-formation were analyzed for their bulk chemistry by a combination of gravimetric, flame photometric, and colorimetric techniques. The results are listed in Table 1. Most samples contain abundant carbonates or silicates, or both. Only samples with a low MnO content (the highest being 2.34 weight percent MnO; analysis 22, Table 1) were selected for bulk chemical analysis and electron microprobe study of the assemblage. The SiO_2, FeO, and Fe_2O_3 values are generally high and variable, and CaO, MgO, and CO_2 are also major and highly variable components (Table 1). The amounts of Al_2O_3, Na_2O, and K_2O are relatively small (maximum Al_2O_3 = 3.95 percent in anal. 5; maximum Na_2O = 1.48 percent in anal. 3; and maximum K_2O = 0.53 percent in anal. 19).

In a study of the assemblage changes of progressively metamorphosed rocks, it is highly desirable to consider an essentially isochemical system. Although the metamorphosed iron-formations south of the Grenville Front (see Fig. 1) may not be exactly isochemical (except for possible loss of *e.g.* H_2O or CO_2, or both) with the unmetamorphosed iron-formations to the north, a comparison of the results in Table 1 with published analyses of unaltered and unmetamorphosed Labrador Trough materials is instructive. Figure 2 shows the chemical distribution, in terms of weight percents of three of the most abundant and variable components (CaO, MgO, FeO), of the unmetamorphosed iron-formations and their metamorphic equivalents. This figure leads to the conclusion that all the iron-formations in the Labrador Trough are represented by a rather limited range of composition, and that indeed the overall

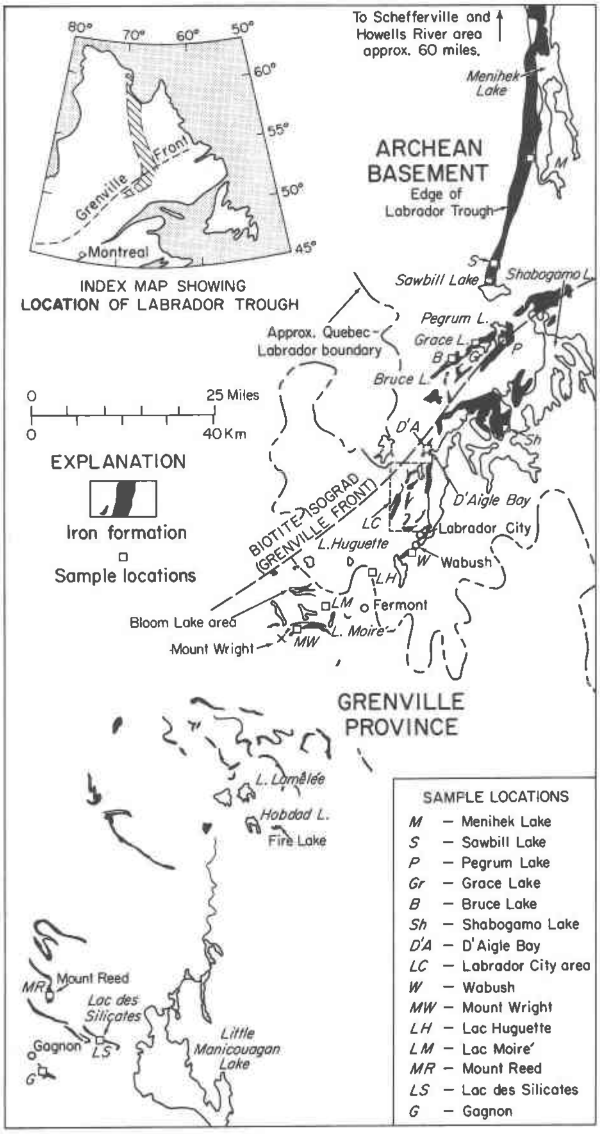

Fig. 1. Proterozoic iron-formation in the southern part of the Labrador Trough (map modified after Gross, 1968). Areas sampled for this study are located and listed in the legend. The location of the biotite isograd, which is the northernmost expression of Grenville metamorphism, is after Fahrig (1967).

[1] Mineral abbreviations are listed in Table 2.

Table 1. Chemical analyses of bulk samples of iron-formation in the Labrador Trough. Explanation for sample locality abbreviations is given in the legend to Fig. 1.

	1(S)[1]	2(P)	3(Sh)	4(D'A)	5(D'A)	6(LC)	7(LC)	8(LC)	9(LC)	10(LC)	11(LC)	12(LC)
SiO_2	24.00	42.35	51.93	44.9	43.6	26.90	36.42	60.60	14.99	46.53	31.95	35.83
TiO_2	trace	trace	trace	0.29	0.55	trace	trace	0.10	trace	trace	trace	trace
Al_2O_3	0.44	0.80	0.27	2.62	3.95	0.21	0.20	0.05	0.07	0.07	0.76	0.32
Fe_2O_3	0.93	2.86	30.77	none[2)]	21.3	3.90	43.05	20.86	76.86	47.44	11.42	18.86
FeO	16.52	15.88	10.76	29.6	13.5	19.92	18.32	12.34	5.30	1.08	33.72	31.41
MnO	0.87	0.62	0.35	1.03	0.81	1.42	0.17	0.28	0.12	0.59	0.59	0.64
MgO	10.30	8.50	3.62	4.45	3.30	7.27	0.48	1.06	0.57	3.46	7.17	7.78
CaO	15.30	10.40	0.10	1.47	4.63	9.89	0.24	0.83	0.73	0.04	4.02	0.07
Na_2O	0.03	0.03	1.48	0.026	1.18	0.13	0.05	0.05	0.03	0.03	0.06	0.04
K_2O	0.02	0.04	0.07	0.20	0.41	0.05	0.05	0.02	<0.02	<0.02	0.03	0.05
$H_2O(+)$	0.15	0.30	0.22	0.93	0.43	0.12	0.19	0.09	1.13	0.34	9.66	0.62
$H_2O(-)$	0.05	0.30	0.00	0.09	0.04	0.00	0.00	0.02	0.09	0.00	0.07	0.10
P_2O_5	0.05	0.04	<0.02	0.054	0.12	<0.02	<0.02	<0.005	0.02	trace	0.05	0.04
CO_2	31.57	17.49	0.03	13.4	6.50	29.79	0.42	3.88	0.06	0.05	0.38	3.99
S	0.006	0.14	<0.02	0.028	0.005	<0.02	<0.02	<0.001	0.036	0.078	0.034	0.052
C	trace	0.02	<0.02	0.54	0.12	<0.02	<0.02	n.d.[3)]	<0.02	<0.02	<0.02	<0.02
Total	100.236	99.77	99.66	99.628	100.445	99.66	99.65	100.186	100.046	99.748	99.934	99.822

	13(LC)	14(LC)	15(LC)	16(LC)	17(LC)	18(LC)	19(LC)	20(MR)	21(MR)	22(MR)	23(MR)
SiO_2	16.65	50.76	45.04	43.08	47.42	37.81	45.66	62.3	56.5	38.8	12.9
TiO_2	0.21	0.10	0.09	0.12	0.07	0.07	0.27	none[2)]	none[2)]	0.010	0.038
Al_2O_3	0.17	0.04	0.02	0.26	0.20	0.19	3.32	none[2)]	0.86	0.66	none[2)]
Fe_2O_3	8.43	1.85	1.48	10.62	1.64	3.02	2.22	4.51	1.88	10.2	28.1
FeO	19.35	21.57	15.47	23.50	15.74	20.10	39.14	27.0	33.0	40.4	22.7
MnO	1.85	1.10	1.07	1.01	0.43	0.52	2.17	0.70	1.19	2.34	0.46
MgO	9.50	6.28	6.30	7.55	8.65	7.50	5.31	1.99	3.79	5.69	9.38
CaO	13.07	6.65	11.36	6.64	19.14	18.21	0.04	1.34	0.64	0.64	10.6
Na_2O	0.07	0.05	0.09	0.05	0.23	0.13	0.26	none[2)]	0.23	0.04	<0.01
K_2O	0.10	0.02	0.03	0.02	0.02	0.03	0.53	0.02	0.25	0.02	0.02
$H_2O(+)$	0.28	0.94	0.48	1.18	0.46	1.21	0.84	0.13	0.16	0.16	0.07
$H_2O(-)$	0.03	0.02	0.03	0.08	0.14	0.03	0.00	0.061	0.044	0.056	0.19
P_2O_5	0.088	0.057	0.083	0.07	0.06	0.07	trace	0.029	0.094	0.073	0.027
CO_2	30.04	10.50	18.40	5.80	5.60	10.60	0.05	1.82	1.75	0.90	15.5
S	0.052	0.002	0.002	0.11	0.014	0.39	0.083	0.004	0.017	0.002	0.004
C	n.d.[3)]	n.d.[3)]	n.d.[3)]	n.d.[3)]	n.d.[3)]	n.d.[3)]	<0.02	0.09	0.13	none[2)]	0.17
Total	99.89	99.939	99.945	100.09	99.814	99.88	99.913	99.994	100.535	99.991	100.169

1) Abbreviations for sample locations shown in Fig. 1; 2) none = not detected; 3) n.d. = not determined. Analyses 1,2,3,6,7,9,10,11,12, and 19 by Hiroshi Haramura, analyses 8,13,14,15,16,17 and 18 by Koichi Mizubayashi, both of the Tokyo Institute of Technology, Tokyo, Japan; analyses 4,5,20,21, 22 and 23 by Maynard Coller, Indiana University, Bloomington, IN. Mineral abbreviations listed in Table 2; mineral name in parentheses means trace amount; mineral listing in decreasing relative abundance.

1(S), no. 3: ch-dol-sid. 2(P), no. 1: qtz-dol-gru-(goeth). 3(Sh), no. 2: qtz-mag-Mgrieb-(talc). 4(D'A), Y350A: sid-gru-qtz-alm-stilp-"rip"-mag-(py). 5(D'A), Y483C: qtz-mag-dol-alm-bio-ab-tour. 6(LC), Y1027C: ank-sid-qtz. 7(LC), C656: qtz-mag-dol-hem. 8(LC), Humphrey Mine: qtz-mag-(sid)-(ank). 9(LC), C675: qtz-spec-mag-dol(to ank). 10(LC), Smallwood Mine: qtz-spec-anth-(mag). 11(LC), Smallwood Mine: eu-ank-gru-mag-qtz. 12(LC), Y1018C: gru-mag-ank. 13(LC), Carol Mine 7c: Fedol-sid-qtz-mag-phlog-"rip". 14(LC), Humphrey Mine: qtz-gru -ank. 15(LC), Carol Mine 9A: ank-gru-qtz. 16(LC), Wabush 7, no. 7: gru-qtz-mag-cal. 17(LC), Wabush no. 4, 18a: qtz-ferrosal-gru-cal. 18(LC), Luce 2G: gru-act-ferrosal-mag-cal-(py). 19(W), Wabush Mines, 623: eu-alm-bio-mag-(gru)-(sid). 20(MR), K-13: eu-qtz-mag-ank. 21(MR), L2: eu-alm-ab-qtz-mag-bio-(py). 22(MR), L3: eu-alm-mag-ank-qtz-(ab). 23(MR), M8: dol-mag-qtz-(sid)-(py).

chemistries (discounting SiO_2, H_2O, and CO_2) of the unmetamorphosed and metamorphic iron-formations are essentially the same. Hence we may assume that the metamorphic reactions took place in an essentially isochemical system, except for probable loss of volatile components such as H_2O and CO_2.

Iron-formation assemblages as a function of metamorphic grade

Table 2 lists assemblages in the iron-formations of the Labrador Trough and in closely associated rock types, as sampled at the various localities shown in Figure 1. A graphical representation of the iron-formation assemblages in terms of molecular percentages of CaO, MgO, and (FeO+MnO) is given in Figure 3. Because almost all the assemblages contain quartz, these diagrams represent SiO_2-saturated assemblages. H_2O and CO_2 are tentatively, for the purposes of the graphical illustrations, considered as perfectly mobile components (μH_2O and μCO_2 arbitrarily fixed by an external system). The total Fe in the various minerals is recalculated as FeO. This is undoubtedly correct for all the carbonates and the majority of the silicates in the iron-formation assemblages. The small amount of MnO in each of the mineral analyses is summed with FeO, because Mn^{2+} and Fe^{2+} tend to substitute for each other in the same structural sites in the carbonates and silicates. Minerals with considerable Al_2O_3 contents, such as almandine, biotite, chlorite ("ripidolite"), and hornblende have also been plotted in Figure 3, but tielines to these minerals are dashed because their compositions do not lie in the plane of projection.

The mineral assemblages of the unmetamorphosed (probably late diagenetic) iron-formation assemblages in the central part of the Labrador Trough from the Howells River area, and the Menihek, Sawbill, Grace, and Bruce Lake regions are given in the upper left part of Table 2. Similarly detailed assemblage and chemical information is given by Floran and Papike (1975, 1978) for the low- and high-grade contact metamorphic rocks of the Gunflint Iron Formation, and by French (1968) for contact-metamorphosed rocks of the Biwabik Iron Formation. The variety and excellent preservation of the various iron-formation types (*e.g.* sulfide, silicate, carbonate–magnetite, and carbonate–hematite; see James, 1954, and Klein and Fink, 1976) in the Howells River area is unique for the central and southern part of the Labrador Trough. In the localities of Menihek, Sawbill, Grace, and Bruce Lakes the author has located mainly extensive carbonate occurrences, with an additional oxide type at Grace Lake only. The unmetamorphosed assemblages are shown graphically in Figures 3.1 to 3.10. These consist mainly of chert, one or two carbonates (siderite or ferroan dolomite or ankerite, or both species), minor amounts of stilpnomelane (*e.g.* Bruce), and traces of a very fine-grained chlorite. This is referred to as "ripidolite", which is an Fe- and Al-rich chlorite in the terminology of Hey (1954). Its composition is the same as that of a possible chamosite, but because the chloritic material is present only in very small to trace amounts, it could not be studied by X-ray diffraction methods. The name "ripidolite" is put in quotation marks throughout because of the uncertainty of whether it is truly a normal 14A chlorite, or 7A septechlorite such as chamosite. A small amount of talc was found in a qtz–mag–hem–talc assemblage from Menihek Lake, but minnesotaite was not found

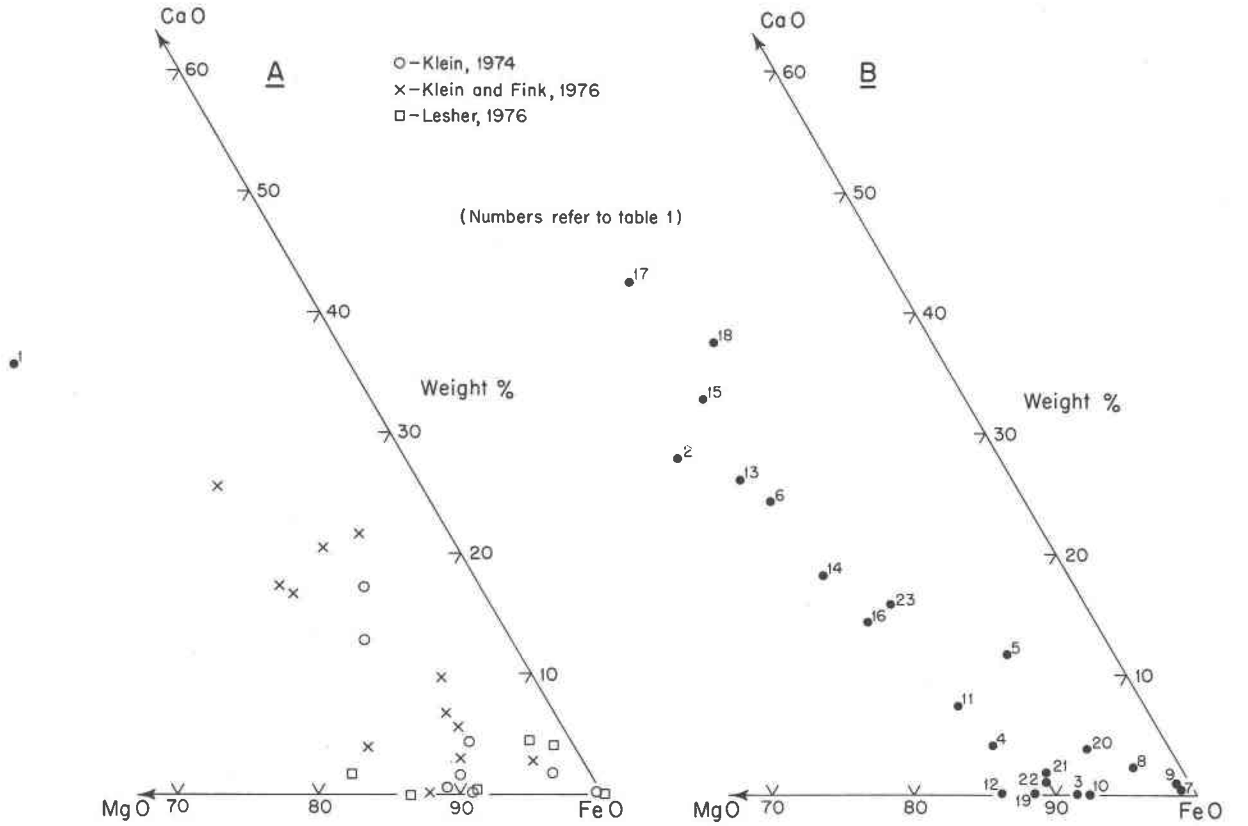

Fig. 2. Bulk chemical analyses of unmetamorphosed (A) and metamorphosed iron-formations (B) in the Labrador Trough, in terms of weight percent CaO, MgO, and FeO (all Fe recalculated as FeO).

Table 2. Listing of assemblages in iron-formations in the Labrador Trough and of some closely associated rock types. ([1]*HR* refers to Howells River area; Klein and Fink, 1976.) Explanation for sample locality abbreviations is given in the legend to Fig. 1. Assemblages containing hematite (or specularite) are grouped below magnetite- (or pyrrhotite-, or pyrite-) containing assemblages within each locality listing.

Locality	Assemblages
HR[1]	qtz-ank-sid-stilp-mag-minn
	green-mag-minn-cal-sid-qtz
	green-stilp-minn-ank-mag-sid-ch
	qtz-mag-sid-dol±hem±ab
	qtz-mag-hem-sid-"rip"-stilp
	mag-hem-dol-stilp-ch
	sid-cal-mag-ch±hem
	} representative assemblages only; more complete listing in Klein and Fink(1976), and Klein(1974).
M	sid-qtz-(py)
	ch-Fedol-py
	ch-mag-hem-talc
	qtz-mag-hem-Fedol-sid-("rip")
	ch-hem-"rip"
	ch-hem-dol-("rip")
S	ch-sid-(py)
	sid-dol-ch-(py)-lim*
	ch-sid-ank
	ch-dol-sid
	ch-sid-("rip")-(py)
Gr	qtz-sid-ank
	Fedol-qtz-sid
	qtz-sid-musc
	qtz-hem-mag-musc-(ap)
B	qtz-ank-stilp-(py)±goeth*
	qtz-sid-Fedol
	Fedol-qtz
	qtz-mag-ank-sid-stilp-goeth*-("rip")
	Fedol-qtz-stilp
	qtz-ank-stilp-("rip")-(goeth)*
	qtz-sid-stilp-("rip")
	(Fedol-ank)-sid-qtz-stilp-goeth*
	qtz-musc schist
P	qtz-Fedol-sid-("rip")
	qtz-Fedol-gru-(goeth)*
D'A	qtz-sid-gru-(cal)
	qtz-mag-sid-gru
	qtz-ank-sid-mag
	qtz-Fedol-mag-("rip")
	qtz-sid-gru-po-mag-"rip"
	alm-sid-qtz-stilp-"rip"-gru-(mag)-(po)
	qtz-sid-alm-bio-po-"rip"-mag
	alm-gru-qtz-po
	qtz-gru-bio
	qtz-mag-dol-hem-tour-phlog-talc
	qtz-dol-mag-bio-alm-ab-tour-hem
	qtz-hem-Fedol-mag
	qtz-mag-hem-Femagnes-tour-"rip"
	qtz-mag-hem-Mndol-"rip"
Sh	qtz-Mgrieb-mag-(hem)-(talc)
LC	qtz-ank-sid-(mag)
	gru-mag-ank-qtz
	ank-gru-qtz
	eu-ank-gru-mag-qtz
	Fedol-sid-qtz-mag-bio-"rip"
	qtz-mag-sid-ank
	Fedol-qtz-mag-bio-"rip"-(po)
	act-gru-ferrosal-mag-cal-(qtz)-(po)
	gru-qtz-mag-cal
	qtz-ferrosal-mag
	qtz-mag-Fedol-hem
	qtz-hem-mag-Fedol to ank
	qtz-spec-anth
	qtz-musc-alm-staur-ky-tour } (Klein, 1966)
	qtz-musc-bio-olig-micr-ky
W	eu-alm-sid-bio-(mag)-(gru)
MW	qtz-hbld(to Al trem)-mag-hem-phlog-cal
	qtz-cumm-hbld-alm
	qtz-hbld-alm-bio-andes(Ab_{68})-mag-py
	qtz-musc-(hem)
	qtz-musc-bio-olig(Ab_{80})-tour-(py)-(po)-(cp)
	alm-hbld-bio-qtz-cal-("rip")-(hem)-(mag)
LH	eu-gru-ferrosal-po-(qtz)
	qtz-eu-ferrosal-po
	ferrohyp-gru-(qtz)-(po)
	eu-ferrosal-hbld-gru-(qtz)
LM	ferrohyp-sid-dol-py-(qtz)
	qtz-eu-cal-po
	ferrohyp-ank-sid-alm-bio-mag-(py)-(qtz)
	qtz-ferrohyp-dol-sid-gru-mag-(po)-(cp)
	qtz-hem-dol-trem
	qtz-gru-alm-dol-cal-bio-po-(cp)
	cal-phlog-qtz
MR	qtz-eu-cal-ank-mag
	qtz-bronz-trem-mag-dol-magnes
	hyp-sal-mag-dol-cal-qtz
	eu-qtz-mag
	qtz-mag-bronz
	eu-alm-ab-qtz-mag-bio-(py)
	eu-alm-qtz-mag-po
	dol-ferrohyp-mag-po
	dol-ferrohyp-mag-cal-qtz
	eu-qtz-mag-ank
	eu-alm-mag-ank-qtz-(ab)
	dol-mag-qtz-sid-(py)
	eu-alm-gru-mag-ank
	eu-mag-ank-bio-(qtz)
	qtz-mag-ferrohyp-gru-cal
	eu-mag-cal-ank-qtz
	qtz-orthofer-(mag)
	eu-sid-gru-bio-qtz-mag-(py)
	eu-cal-qtz-mag
	qtz-mag-sal-dol-cal-(spec)
	qtz-mag-spec-dol-cal
	qtz-spec-anth-talc-(mag)
	qtz-olig(Ab_{74})-micr-bio
LS	eu-ank-cal-gru-bio-qtz-alm-mag±po
	eu-gru-cal-po-(qtz)
	ank-ferrohyp-mag-(qtz)
	gru-eu-po-(qtz)-(cp)-(mag)
G	qtz-diop-dol-trem-spec
	dol-trem-qtz-spec-ep
	cal-dol-trem-diop-phlog-qtz-(ep)-(spec)
	cal-diop-trem-dol-qtz-spec
	qtz-spec-phlog-ep-ap
	dol-spec-tour-qtz
	dol-cal-spec-hbld-phlog-qtz
	qtz-musc-spec
	cal-diop-trem-spec-mag-qtz
	qtz-spec-mag-phlog-micr
	qtz-diop-trem-cal-(talc)
	qtz-spec-phlog-tour-ep-ap-(musc)-(ky)
	qtz-olig(Ab_{72})-bio-musc-chlor-(mag)-(po)
	qtz-andes(Ab_{67-70})-micr-bio-musc-alm-chlor-po-hbld-(cp)
	qtz-micr-bio-alm-musc-chlor-(po)

Mineral abbreviations:

ab-albite	cp-chalcopyrite	hbld-hornblende	orthofer-orthoferrosilite
act-actinolite	cumm-cummingtonite	hem-hematite	phlog-phlogopite
alm-almandite	diop-diopside	hyp-hypersthene	po-pyrrhotite
Altrem-Al tremolite	dol-dolomite	ky-kyanite	py-pyrite
andes-andesine	ep-epidote	lim-limonite	qtz-quartz
ank-ankerite	eu-eulite	mag-magnetite	"rip"-"ripidolite"
anth-anthophyllite	Fedol-ferroan dolomite	magnes-magnesite	sal-salite
ap-apatite	Femagnes-ferroan magnesite	Mgrieb-Mg riebeckite	sid-siderite
bio-biotite	ferrohyp-ferrohypersthene	micr-microcline	spec-specularite
bronz-bronzite	ferrosal-ferrosalite	minn-minnesotaite	staur-staurolite
cal-calcite	goeth-goethite	Mndol-manganoan dolomite	stilp-stilpnomelane
ch-chert	green-greenalite	musc-muscovite	tour-tourmaline
chlor-chlorite	gru-grunerite	olig-oligoclase	trem-tremolite

*Sequence of mineral listing is in decreasing relative abundance. Parentheses means trace amount. * signifies secondary alteration. Assemblages in italics represent rock types closely associated with the iron-formations.*

in any of the iron-formation occurrences at Menihek, Sawbill, Grace, or Bruce Lakes. This is in contrast to the pervasive occurrence of minnesotaite in the carbonate and silicate types of iron-formation in the Howells River area (Klein, 1974; Klein and Fink, 1976) and elsewhere (*e.g.* James, 1955; French, 1968). Talc has also been reported by Lesher (1976) from iron-formations 40 miles north of the Howells River area, and by Floran and Papike (1975) in the low-grade metamorphic parts of the Gunflint Iron Formation. Some muscovite-rich qtz–hem–mag assemblages are noted in the Grace Lake area (Table 2), and a quartz–muscovite schist is closely associated with iron-formation in the Bruce Lake region. Small to trace amounts of pyrite are found in several unweathered iron-formations. The various unmetamorphosed assemblages show reasonably similar element partitionings but by no means perfectly parallel tie-lines (Figs. 3.1 to 3.10). The unmetamorphosed assemblages in the Menihek, Sawbill, and Grace Lake localities are fine-grained, with abundant chert and well-preserved granule, and, in places, oolitic textures. In the Bruce Lake locality pervasive small-scale shearing is present.

The first mineralogic evidence of metamorphism in the iron-formation is found in the Pegrum Lake area, where the biotite isograd crosses the iron-formation (Fig. 1). Here the iron-formation shows the first development of fine-grained grunerite[2] (Fig. 3.11) in a highly sheared qtz–Fedol–gru assemblage. Southwardly from the biotite isograd (Fig. 1) the metamorphic grade of the iron-formation and associated rock types increases rather rapidly. In the D'Aigle Bay region coarse-grained almandine-rich garnets (Fig. 3.13) are common, and the grunerite is of a considerably larger grain size than at Pegrum Lake. Clearly the garnet isograd is located north of D'Aigle Bay but south of the biotite isograd in the Pegrum Lake area. Hydrous iron-rich silicates such as "ripidolite" and stilpnomelane are still present in the D'Aigle Bay area, and abundant siderite, dolomite–ankerite, and minor amounts of calcite are also found. Small amounts of biotite or phlogopite, tourmaline, and in one instance talc are present in some of the hematite-containing assemblages. The Mg/(Mg+Fe+Mn) content of grunerite is always slightly greater than that of coexisting siderite, and the siderite has a slightly higher Ca/(Ca+Fe+Mn) ratio than the coexisting grunerite. In all occurrences of almandine–grunerite, the Mg/(Mg+Fe+Mn) of the grunerite is considerably higher than that of the almandine. The grunerite- and almandine-containing assemblages in the D'Aigle Bay region have a distinctly metamorphic texture, with locally pronounced grunerite lineations. However, the banded quartz-oxide and quartz–carbonate±oxide assemblages appear essentially unmetamorphosed except for strong recrystallization textures.

In the Labrador City, Bloom Lake, and Mount Wright areas various types of amphiboles and amphibole pairs become abundant in the iron-formations and associated rock types. Amphibole-rich assemblages from the sequences that underlie the ore horizons in the Labrador City area have been described by Klein (1966). For the Bloom Lake area, Mueller (1960) gives detailed chemical data (obtained by spectrographic techniques) on a large number of amphiboles (mainly actinolite and members of the cummingtonite–grunerite series; many of these occur as pairs) and lesser Ca-pyroxenes. A graphical compilation and discussion of these silicate data are given in Klein (1968) and Immega and Klein (1976). The metamorphic grade of the Labrador City area is in the kyanite–staurolite zone, on the basis of pelitic schist assemblages closely associated with the iron-formation (Klein, 1966). Because of the generally similar amphibole-rich assemblages in the Labrador City, Bloom Lake, and Mount Wright areas, all three areas probably underwent similar metamorphic conditions. The garnet, staurolite, and kyanite isograds must be crowded rather closely together in an area immediately to the northwest of the Labrador City or Bloom Lake regions, because the biotite isograd occurs at only approximately 2 miles NW of the northern part of the Labrador City region (see Fig. 1).

In the iron-formations of the Labrador City and Bloom Lake areas, pyroxenes are very much subordinate to amphiboles. Members of the dolomite–ankerite series, and siderite and to a lesser extent calcite, are commonly present. Biotite or phlogopite occur in some sporadic assemblages, and "ripidolite" occurs as a minor to trace constituent. The assemblages for the Labrador City and Mount Wright areas are listed in Table 2 and shown graphically in Figures 3.14 to 3.17. The Labrador City and Bloom Lake area assemblages represent carbonate, carbonate–silicate, and silicate iron-formation, but in the Mount Wright region such iron-formation assemblages are completely lacking. Whereas the iron-formation in the Labrador City region is a rather regularly layered

[2] Grunerite refers to Fe–Mg clinoamphiboles with Fe > Mg (atomic percent); cummingtonite refers to members of the same series with Mg > Fe.

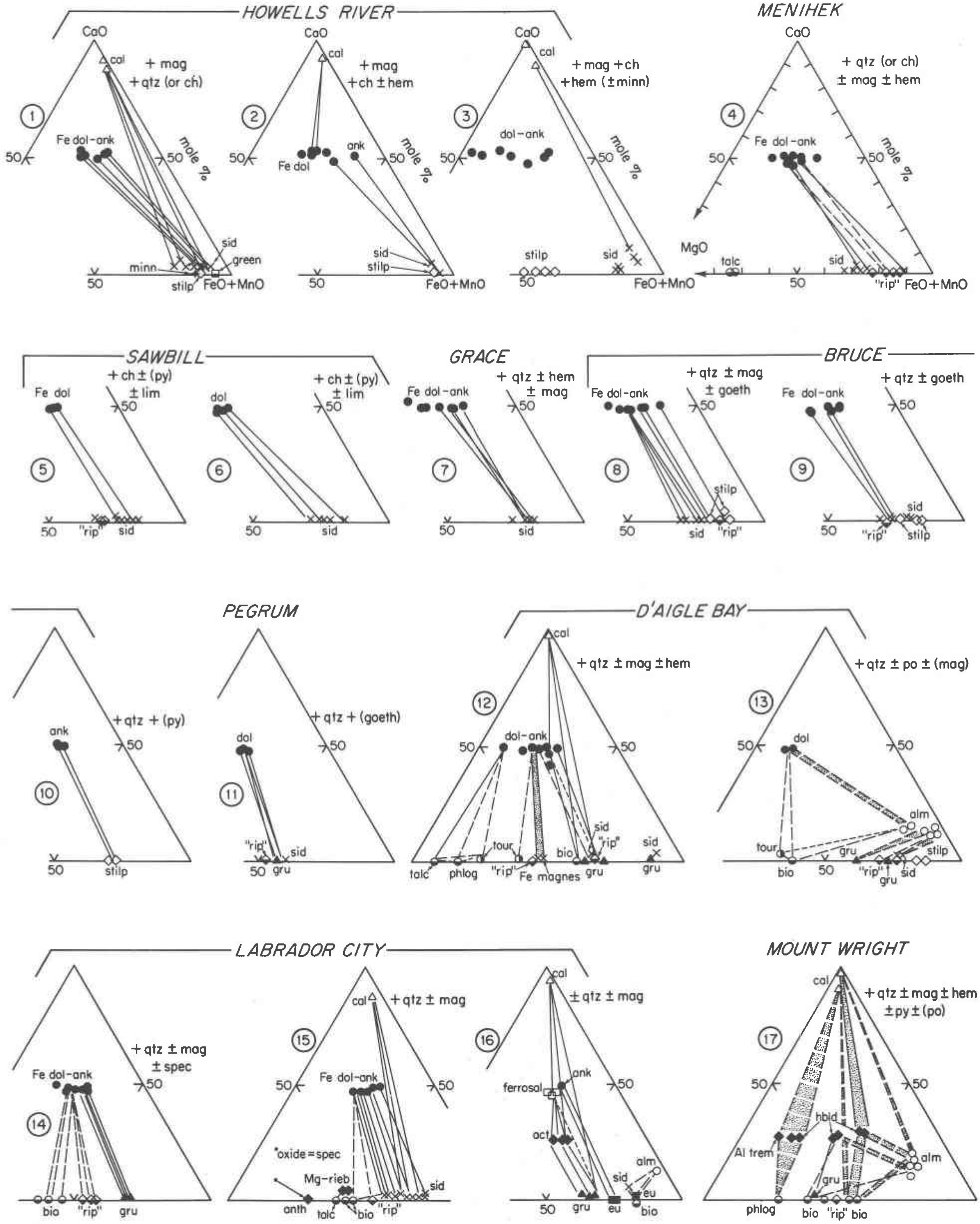

Fig. 3. Graphical representation of assemblages in iron-formations in the Labrador Trough and of some closely associated rock types in terms of molecular percentages of CaO, MgO, and FeO + MnO (all Fe recalculated as FeO). Mineral abbreviations are given in Table 2. Long-dash tielines are used when a mineral composition does not lie in the plane CaO–MgO–(FeO+MnO). Short-dash tielines are used in case of major tieline crossing. Because of the highly reduced scale of the triangles each specific data point can not be represented; instead only a few symbols are shown where many data points cluster. Shaded areas represent regions of many essentially parallel tielines.

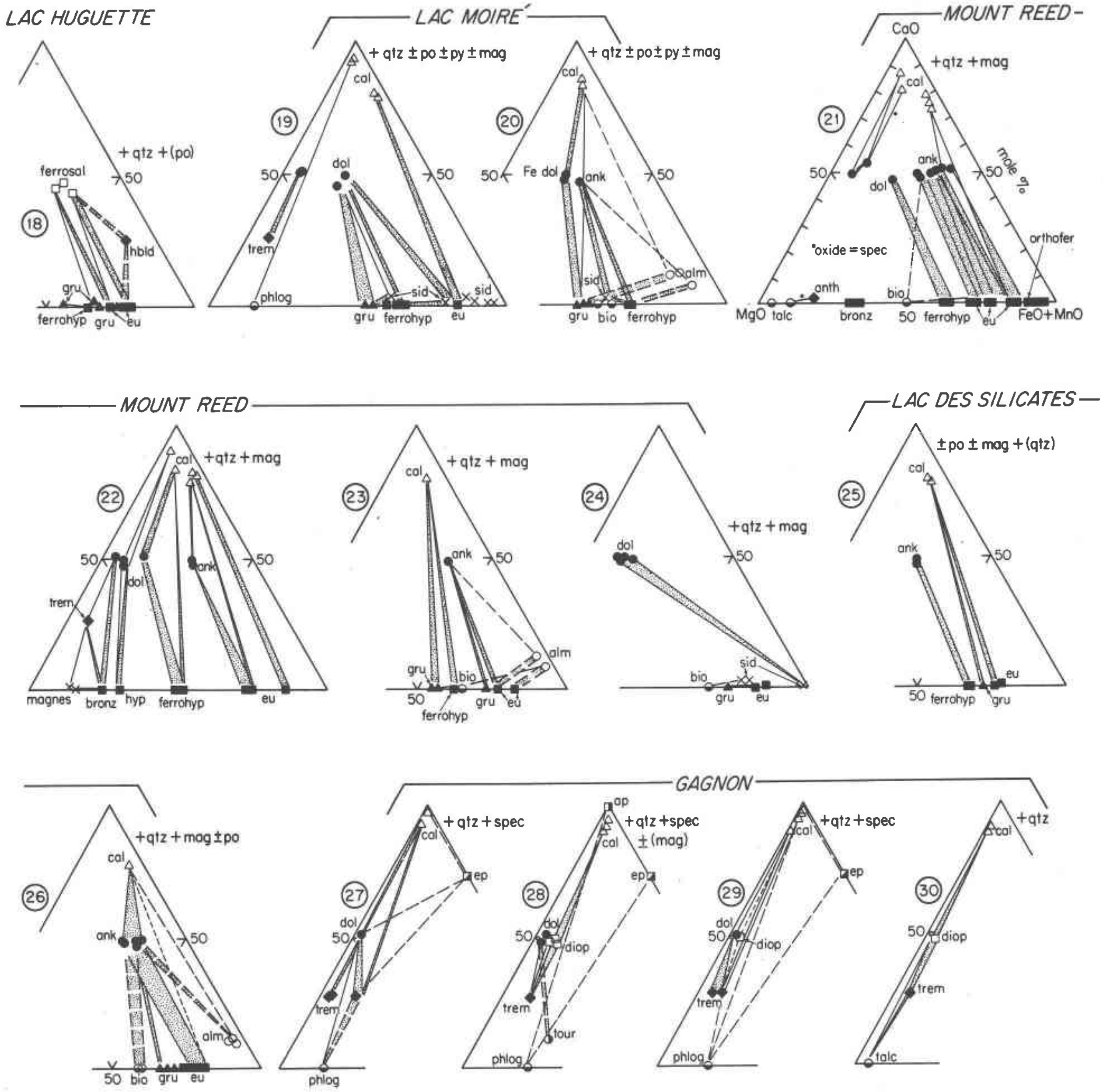

Fig. 3 (continued).

sequence of qtz–spec (at the top), qtz–spec–mag, qtz–mag, qtz–mag–silicate, qtz–mag–carbonate, and quartz–carbonate–silicate (at the bottom), the iron-formation at Mount Wright consists essentially of qtz–spec. A major facies change must have occurred between the Labrador City and Mount Wright area iron-formations during their depositional stages. The majority of assemblages reported for the Mount Wright area, therefore, are from amphibolites and impure quartzites, closely associated with the iron-formation.

Although the element fractionation among the various minerals of the Labrador City iron-formations is reasonably consistent (Figs. 3.14 to 3.16) it is remarkable that for an essentially constant cation bulk composition (in terms of SiO_2, CaO, MgO, FeO, and MnO) but clearly variable CO_2 and H_2O contents, three totally different assemblages are found. For example, the assemblage qtz–ank–sid–(mag) makes up a thick section of the iron-formation sequence (anal. 6, Table 1) in one part of the district, but qtz–ank–gru and qtz–ank–eu–gru are found in nearby

Table 3. Representative electron probe analyses of some siderites and calcites in metamorphic iron-formation

wt%	1	2	3	4	5	6	7	8	9	10	11	12	13	14
FeO	47.78	47.61	53.71	42.55	33.46	47.17	5.15	7.62	10.28	11.09	11.27	10.45	12.18	0.98
MnO	1.66	1.66	0.96	6.49	7.58	3.57	1.16	1.37	3.14	3.10	2.01	1.77	2.49	0.30
MgO	7.84	7.47	3.30	6.17	14.07	6.96	1.37	2.86	1.57	2.31	2.01	2.78	1.87	4.66
CaO	1.30	0.96	1.20	2.83	2.01	1.47	46.92	50.70	45.51	44.44	42.22	43.10	38.79	56.19
Recalculated on the basis of 2(Fe,Mn,Mg,Ca)														
Fe	1.468	1.492	1.730	1.335	0.973	1.450	0.150	0.193	0.276	0.295	0.318	0.289	0.360	0.024
Mn	0.052	0.053	0.031	0.206	0.223	0.111	0.034	0.035	0.085	0.083	0.057	0.050	0.074	0.007
Mg	0.429	0.417	0.189	0.345	0.729	0.381	0.071	0.129	0.075	0.109	0.101	0.137	0.098	0.204
Ca	0.051	0.039	0.050	0.114	0.075	0.058	1.745	1.643	1.564	1.513	1.524	1.525	1.467	1.765

ASSEMBLAGES. 1 D'A: alm-sid-qtz-stilp-"rip"-gru-(mag)-(po). 2 D'A: qtz-sid-alm-bio-"rip"-(py)-(mag). 3 D'A: qtz-mag-sid-gru. 4 W: eu-alm-sid-bio-(mag). 5 LM: qtz-ferrohyp-dol-sid-gru-mag-(po)-(cp). 6 MR: eu-sid-gru-bio-qtz-mag-(py). 7 LC: gru-qtz-mag-cal. 8 LM: qtz-gru-alm-dol-cal-bio-po-(cp). 9 LM: qtz-eu-cal-po. 10 LS: eu-ank-cal-gru-bio-qtz-alm. 11 LS: eu-ank-cal-gru-bio-qtz-alm-mag. 12 MR: eu-mag-cal-ank-qtz. 13 MR: qtz-eu-cal-ank-mag. 14 G: qtz-diop-trem-cal-(talc).

sequences (within a mile of each other, or sometimes within several hundred feet) (Figs. 3.15, 3.16). Similarly, qtz–dol–sid assemblages occur near a compositionally equivalent ferrosal–act–gru occurrence (Figs. 3.15, 3.16). Such assemblage inconsistencies are undoubtedly related to the less than perfectly mobile behavior of volatile components such as CO_2 and H_2O, discussed later.

A very Fe^{3+}-rich assemblage is represented by qtz–spec–anth (Fig. 3.15; anal. 10, Table 1), and a rather uncommon Na-rich assemblage from the nearby Shabogamo Lake area, consisting of qtz–Mgrieb–mag–(hem)–(talc) (anal. 3, Table 1), is also shown in Fig. 3.15. Fig. 3.16 also shows the assemblage eu–alm–sid–bio–mag–(gru) from Wabush Mines, which is located only about two miles south of Labrador City. In the Wabush Mines area pyroxene- and pyroxenoid-rich (rhodonite) assemblages tend to be abundant locally. This is in contrast to the assemblages in the Labrador City, Bloom Lake, and Mount Wright areas, which contain abundant hydrous silicates such as grunerite, actinolite, and micas. The grain sizes of these rocks are medium- to coarse-grained with frequently well-developed schistose textures. Original sedimentary banding is still preserved, but granule textures occur only sporadically and are poorly defined.

The iron-formations in the Lac Huguette and Lac Moiré areas appear to be transitional in mineralogy between those of the Labrador City–Bloom Lake–Mount Wright and Mount Reed–Lac des Silicates regions. At Lac Huguette and Lac Moiré pyroxenes occur in great abundance, but amphiboles are also present. The carbonates are represented by siderite, dolomite–ankerite, and calcite. The assemblages for these two localities are listed in Table 2 and shown in Figures 3.18 to 3.20. As was also observed in the assemblages at D'Aigle Bay, grunerite is more Mg-rich than the coexisting siderite, and the siderite is slightly more calcic than the grunerite. The siderite compositions in these assemblages (Table 3) are somewhat more Ca-rich than any siderites encountered in the unmetamorphosed assemblages. It is possible that an original (Fe,Mg) siderite with only minor amounts of Ca reacts to form the various Fe–Mg silicates (*e.g.* ferrohypersthene, eulite, grunerite), with the remaining siderite somewhat enriched in Ca. This is borne out by the mineral distributions in Figures 3.19 and 3.20. In orthopyroxene–grunerite coexistences grunerite always has a higher MgO/FeO ratio than the coexisting orthopyroxene, as was shown also by Kranck (1961) and Butler (1969).

The iron-formation assemblages at Mount Reed and Lac des Silicates, which represent rather similar bulk compositions, have been studied by Kranck (1961) and Butler (1969). The majority of assemblages from these areas consist predominantly of anhydrous minerals such as quartz, members of the orthopyroxene series, carbonates and magnetite (Table 2; Figs. 3.21 to 3.26). Clinopyroxenes of salite to ferrosalite composition, and clinopyroxene–orthopyroxene pairs, are common in these regions. A graphical compilation of all reported pyroxene compositions is given in Immega and Klein (1976). Orthopyroxene-rich iron-formation assemblages from elsewhere have also been described by Bonnichsen (1969) and Simmons *et al.* (1974). The orthopyroxene compositions in this study range from bronzite to orthoferrosilite. The most Fe-rich orthoferrosilite (Table 4) occurs in an orthofer–mag–qtz assemblage with, on the basis of nine averaged analyses, an Fe/(Fe+Mg+Mn) = 0.947 and an Fe/(Ca+Fe+Mg+Mn) = 0.937 [the total range of compositions is from 0.917 to 0.956 for the Fe/(Ca+Fe+Mg+Mn)ratio].

A similarly Fe-rich orthoferrosilite occurrence is reported by Jaffe *et al.* (1978) in a pyroxene gneiss. Grunerite is generally present in only minor amounts, and consistently has a higher MgO/FeO ratio than coexisting orthopyroxene. Siderite was found in only two Mount Reed iron-formation assemblages, but calcite and members of the dolomite–ankerite series are common (Fig. 3.24). In the eu–sid–gru–bio–qtz–mag–(py) assemblage the siderite has a considerably higher CaO/(FeO+MnO) ratio than the coexisting grunerite or eulite (this was noted for D'Aigle Bay, Lac Huguette, and Lac Moiré assemblages as well). The other siderite-containing assemblage, dol–mag–qtz–sid–(py), is remarkable because it contains no iron-silicates, as would have been expected by analogy with the other assemblages. This assemblage also illustrates that CO_2 has not behaved as a perfectly mobile component. Magnesite occurs in one Mount Reed assemblage that consists of qtz–bronz–trem–mag–dol–magnes (Fig. 3.22). One very Fe^{3+}-rich assemblage consists of qtz–spec–anth–talc–(mag) (Fig. 3.21), and is very similar to one from Labrador City (Fig. 3.15). The assemblages from Lac des Silicates (Table 2; Figs. 3.25, 3.26) are qualitatively very similar to those of Mount Reed. The calcites in many of these assemblages are very iron-rich, with a maximum FeO content of 12.18 weight percent in a qtz–eu–cal–ank–mag assemblage from Mount Reed (Table 3, anal. 13). The textures of the rocks from the Mount Reed and Lac des Silicates areas are equigranular, medium- to coarse-grained, and show pronounced mineralogic banding which probably represents relict sedimentary features.

The Gagnon region contains the most coarse-grained rocks of any in this study. The ore horizons, in the now-closed Lac Jeanine Mine, consist of only two minerals, very coarse-grained equigranular quartz and specularite. Specularite-rich bands, especially in the tight crests of folds, may show individual specularite grains 1 cm in diameter. Quartz grains in associated quartzite are of a similar size. The occurrence of small amounts of kyanite in associated rock types (Table 2) indicates that the general metamorphic grade is still within the kyanite zone. The iron-formation sequence in the Lac Jeanine mine, of the Gagnon region, is very different from that in, *e.g.* Mount Reed, Lac des Silicates, Lac Huguette, Lac Moiré, or Labrador City. In the Gagnon region the sequences rich in iron-silicates or iron-carbonates are missing, and there is little to no magnetite-containing iron-formation. The only assemblages that are conducive to study are the associated quartzite, which directly underlies and overlies the ore horizons, and associated coarse-grained calc–silicate-rich marbles. The quartzite ranges from monomineralic quartz to qtz–spec–musc assemblages (Table 2) and the marbles show coarse-grained qtz–cal–diop–trem–spec–mag assemblages (others are listed in Table 2). Because of the very low Fe^{2+} content (as reflected by the large amounts of specularite and essentially no magnetite), and also because of the high Ca-content of the marble assemblages, the mineral coexistences plot close to the Mg–Ca side of the triangles (Figs. 3.27 to 3.30), in contrast with the chemical location of most of the previous assemblages. As can be seen, calcite, dolomite, diopside, tremolite, and phlogopite (or muscovite) are common in specularite-containing calc–silicate assemblages. The assemblage in Figure 3.30 consists only of silicates with minor calcite, whereas assemblages of similar bulk composition (Figs. 3.27 to 3.29) contain dolomite, without, for example, diopside, or with only a trace amount of this silicate. As in other deposits discussed above, the CO_2 and H_2O components do not appear to have behaved as perfectly mobile components.

Table 4. Representative analyses of orthopyroxenes in metamorphic iron-formation

wt%	*1*	*2*	*3*	*4*	*5*	*6*
SiO_2	53.36	55.29	50.04	48.01	47.29	45.54
TiO_2	0.00	0.00	0.00	0.00	0.00	0.00
Al_2O_3	0.03	0.02	0.02	0.21	0.16	0.04
FeO	16.32	17.96	34.33	39.56	44.51	53.07
MnO	1.47	1.60	3.89	5.09	2.57	0.42
MgO	28.49	26.03	12.24	7.50	5.41	1.69
CaO	0.31	0.41	0.36	0.64	0.31	0.32
Na_2O	0.00	0.00	0.00	0.05	0.12	0.00
K_2O	0.00	0.00	0.00	0.00	0.00	0.00
Total	99.98	101.31	100.88	101.06	100.37	101.08
Recalculated on basis of 6 oxygens						
Si	1.947	1.996	1.992	1.977	1.987	1.969
Al	0.001	0.001	0.001	0.010	0.008	0.002
Σ	1.948	1.997	1.993	1.987	1.995	1.971
Al	-	-	-	-	-	-
Ti	-	-	-	-	-	-
Fe	0.498	0.542	1.143	1.362	1.564	1.919
Mn	0.045	0.049	0.131	0.178	0.091	0.015
Mg	1.549	1.400	0.726	0.460	0.339	0.109
Ca	0.012	0.016	0.015	0.028	0.014	0.015
Na	-	-	-	0.004	0.010	-
K	-	-	-	-	-	-
Σ	2.104	2.007	2.015	2.032	2.018	2.058
$\frac{Fe}{Fe+Mg+Mn}$	23.80	27.22	57.15	68.10	78.43	93.93
$\frac{Fe}{Ca+Fe+Mg+Mn}$	23.67	27.00	56.72	67.16	77.88	93.24

ASSEMBLAGES. 1 MR: qtz-bronz-trem-mag-dol-magnes. 2 MR: (bronz to hyp)-sal-mag-dol-cal-qtz. 3 MR: qtz-mag-ferrohyp-gru-cal. 4 MR: eu-alm-gru-mag-ank. 5 W: eu-alm-sid-bio-(mag)-(gru). 6 MR: orthofer-mag-qtz.

Metamorphic reactions and conclusions

In the early to late diagenetic assemblages of iron-formation as described by Klein (1974) and Klein

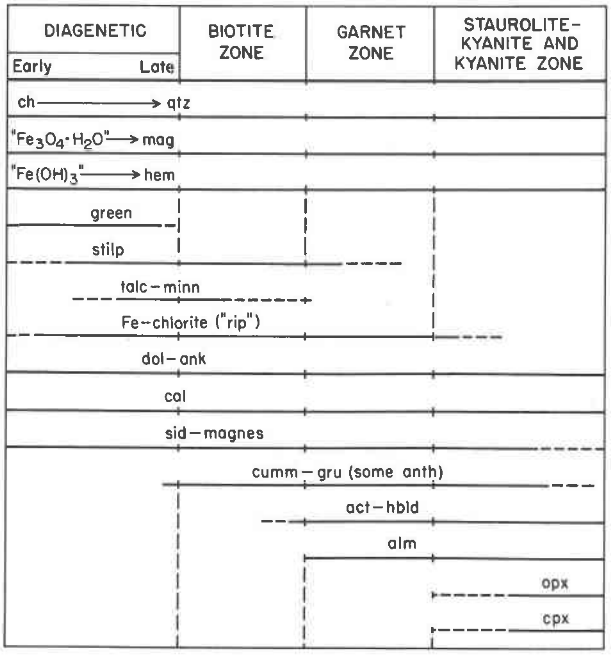

Fig. 4. Relative stabilities of minerals in the regionally metamorphosed iron-formations of the southern part of the Labrador Trough. There are considerable overall similarities in this diagram with the one by James (1955) for the regionally metamorphosed iron-formation of northern Michigan. In the contact-metamorphosed Biwabik Iron Formation (French, 1968, Fig. 23, p. 49) the abundance of the carbonates decreases markedly in the zone rich in orthopyroxene. This holds also for the contact metamorphism of the Gunflint Iron Formation (Floran and Papike, 1978).

and Fink (1976), it is feasible to reconstruct texturally well-documented reactions among minerals (*e.g.* greenalite + 4 SiO_2 = minnesotaite + 2 H_2O), because of the persistence of precursor materials as relict minerals. French (1968) and Floran and Papike (1978) were similarly able to deduce rather specific mineral reactions, as based on textures, in the lower grades of contact metamorphism in the Biwabik and Gunflint Iron Formations, respectively. In the iron-formation materials of this study, such textural interpretations are possible up to about the biotite isograd (Pegrum Lake) where, for example, grunerite is clearly a reaction product of Fe-rich carbonate + chert. However, in any of the higher-grade assemblages, which generally exhibit equigranular textures and which contain no unambiguously identifiable relict minerals or textures, mineral reactions cannot be deduced on textural grounds. Quartz, carbonates, and iron oxides are all strongly recrystallized, and they, as well as additional silicates, occur in general as relatively equigranular grains in seemingly equilibrium textures. It is therefore quite impossible to state uniquely what reaction or combination of reactions is, for example, responsible for the formation of members of the orthopyroxene series. Orthopyroxene is clearly not just a simple dehydration product of the cummingtonite–grunerite series; most certainly the various carbonates, quartz, hydrous silicates, and possible magnetite have been involved in its production. Therefore, instead of writing for the higher-grade metamorphic assemblages a series of hypothetical reactions (see *e.g.* Klein, 1973) of which some (but which ones?) will be most important, it is probably more realistic to assess the relative stabilities and abundances of the most common iron-formation minerals as depicted in Figure 4. Quartz (and originally chert), magnetite, and hematite are present from late diagenetic to high-grade metamorphic conditions. Coexisting hem–mag generally do not exhibit textures that might be interpreted as one oxide replacing the other. This leads to the conclusion that these oxide pairs have rather narrowly buffered the μO_2 of iron-formations throughout their diagenetic and metamorphic history. Carbonates are also present throughout the whole diagenetic–metamorphic range, with calcite probably less abundant under late diagenetic than high-grade metamorphic conditions. French (1968) concluded that calcite is more abundant in the most highly contact-metamorphosed part of the Biwabik Iron Formation than it is in lower grades. Members of the dolomite–ankerite series are abundant throughout the whole range of metamorphic conditions. Siderite appears to become a lesser constituent in the highest-grade zone (with abundant orthopyroxene and considerable quartz in most assemblages; see Table 2) although it is very abundant in diagenetic to low- and medium-grade conditions. Quite clearly siderite is a major reactant in the production of iron–silicates. Figures 3.12, 3.13, 3.16, 3.19, 3.20 and 3.24 illustrate that siderite coexisting with grunerite or eulite (see also Table 3) is relatively more Ca-rich than the silicate (or than the original siderites in lower-grade rocks), which may indicate that the Fe–Mg components of the original siderite were preferentially incorporated into the various prograde metamorphic silicates. The question of what prograde reactions limit the stability fields of talc and minnesotaite is still unresolved. Minnesotaite is clearly a late diagenetic to early metamorphic mineral (Klein and Bricker, 1977; Floran and Papike, 1978; French, 1968; James, 1955) but it is generally absent in grunerite-containing assemblages. It is abundant in the Howells River area, but absent in most of the other unmetamorphosed assemblages. As such one does not observe relict minnesotaite giving way to *e.g.* grunerite or orthopyroxene. Gair (1975) describes a few occurrences of porphyroblasts of grunerite in a fine-grained mesh of minnesotaite, as a result of local contact metamorphism of the Negaunee Iron Formation by a diabase. Floran and Papike (1978) found no textural evidence to support the formation of grunerite from minnesotaite in the Gunflint Iron Formation. In this study some talc is still present in the garnet zone (Shabogamo Lake), but otherwise there is no clear evidence of where the stability fields of the talc and minnesotaite series end. Stilpnomelane can exist all the way from diagenetic to garnet-zone conditions (D'Aigle Bay) and "ripidolite"-type chlorite is present from diagenetic to staurolite–kyanite zone conditions (Labrador City area). Grunerite begins forming at the biotite isograd, and amphiboles in general become very abundant in the garnet and staurolite–kyanite zones (Labrador City–Bloom Lake–Mount Wright areas). Almandine-rich garnet is present in small percentages from the onset of the garnet zone, and remains stable throughout the prograde assemblages in this study. The most likely Al-containing precursor materials for almandine and hornblende are "ripidolite" and stilpnomelane. With increasing temperature, or reduction in μH_2O, or both, pyroxenes (especially orthopyroxenes) become a major constituent (Mount Reed–Lac des Silicates–Gagnon area).

The sequence of mineral stabilities outlined in Figure 4, the assemblage listing in Table 2, and the graphical representations in Figure 3 show in general the accepted sequence of dehydration with increasing metamorphic grade. However, although some geologic units may exhibit a general sequence of decarbonation, decarbonation reactions have been only partial or nonexistent in a considerable number of assemblages and rock types of this study. A picture of continual H_2O and CO_2 loss with increasing metamorphic grade, therefore, is quite inaccurate. On the contrary, CO_2 and H_2O have not behaved as perfectly mobile components, and as such their activities have not been externally controlled [see *e.g.* Ferry (1977) for further discussion]. Indeed, parts of the iron-formations have behaved as almost completely closed systems, whereas closely adjoining parts were essentially open with respect to the behavior of volatile components. Kranck (1961) concluded this for Mount Reed assemblages, and Butler (1969) inferred the existence of μH_2O and μCO_2 gradients on the basis of specific mineral assemblages in the Gagnon area. Similarly, Ferry (1976) concludes that rather large gradients exist in fCO_2 and fH_2O during metamorphism on a bed-to-bed scale in metamorphosed calcareous sediments. The presence of steep gradients in the activities of volatile components such as H_2O and CO_2 between closely adjoining iron-formation assemblages makes a graphical assessment of assemblages with the assumption of complete mobility of *e.g.* CO_2 and H_2O (as was presumed for the construction of Fig. 3) untenable. Indeed, Figure 3 not only shows several tieline crossings, but more importantly it shows carbonate-rich *vs.* silicate-rich assemblages of essentially the same bulk composition coexisting in nearby rocks at constant T and P conditions. This means that the original and local bulk chemical composition (including all of the inert as well as volatile components, such as O_2, H_2O, and CO_2) determines to a very large extent the final assemblage coexistences as well as the compositions of the various minerals. This causes a relatively simple bulk chemical system (iron-formations are often referred to as simple chemical systems) to produce a large and unpredictable array of assemblages with increasing metamorphic grade. The presence of minor components such as Al_2O_3, K_2O, Na_2O increases this complexity further.

The temperature and pressure range of metamorphic conditions is represented at the low end of the scale by assemblages in the Howells River, Menihek, Sawbill, and Bruce Lake areas whereas maximum T and P conditions were probably attained in the Gagnon–Mount Reed–Lac des Silicates areas. Klein and Fink (1976) estimate that the diagenetic assemblages at Howells River represent about 150°C. French (1973) suggests 1 to 2 kbar pressure as a reasonable estimate under such conditions. The highest-grade iron-formation assemblages contain abundant orthopyroxene, magnetite, carbonates, some almandine, and only minor amphiboles. This high-temperature mineralogy is very similar to the highest-temperature assemblages noted by Floran and Papike (1978) in the "orthopyroxene zone" of the contact-metamorphosed Gunflint Iron Formation, immediately adjoining the contact with the Duluth Gabbro. French (1973) describes similar assemblages in the contact-metamorphosed Biwabik Iron Formation, in the zone closest to the Duluth Gabbro Complex. Regionally-metamorphosed iron-formations in southwestern Montana (Tobacco Root Mountains) with very similar, anhydrous, pyroxene-rich assemblages have been studied by Immega and Klein (1976) and Dahl (1977). The various temperature (and pressure)

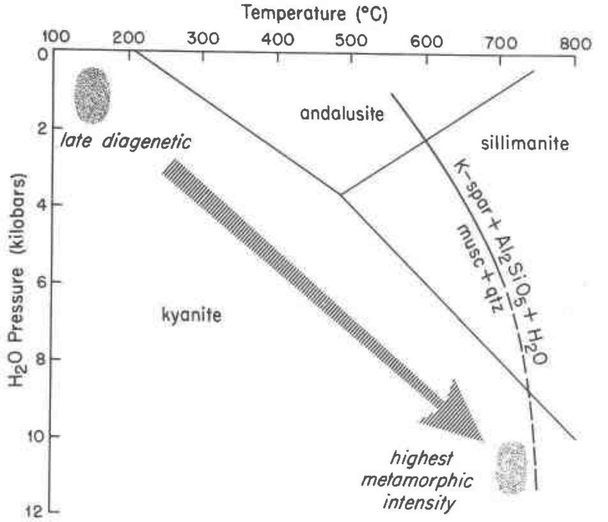

Fig. 5. Temperature–total pressure diagram showing the range of probable conditions of metamorphism for the iron-formation in the southern Labrador Trough. The muscovite breakdown curve is from Chatterjee and Johannes (1974) and the Al_2SiO_5 stability diagram after Holdaway (1971). Because of an average content of about 6.5 weight percent FeO (equivalent to 7.2 weight percent Fe_2O_3) in the naturally occurring muscovite of the highest metamorphic grade area, the region of highest metamorphic intensity is located at a somewhat lower T than the maximum stability curve of pure muscovite (see Velde, 1965).

estimates obtained by the above authors are as follows: Floran and Papike (1978) estimate 840–870°C in the immediate contact zone with the gabbro; French (1968), from experimental results of a quartz–fayalite–magnetite–graphite–vapor equilibrium, suggests that temperatures as high as 800°C could have been reached in the contact zone of the Biwabik Iron Formation; Immega and Klein (1976), from the orthopyroxene–clinopyroxene geothermometer proposed by Ross and Huebner (1975), arrive at an estimated temperature of 650–750°C at 4–6 kbar for the Tobacco Root Mountain iron-formations; Dahl (1977), from a comparative evaluation of various geothermometers as well as oxygen isotope studies of coexisting quartz and magnetite, concludes that peak metamorphic conditions for the essentially anhydrous iron-formations in the Kelly area of southwestern Montana attained 745°±50°C at 6–8.5 kbar. These temperature estimates are relatively similar and cluster about 750°C for such pyroxene-rich iron-formation assemblages. When Ross and Huebner's (1975) orthopyroxene–clinopyroxene geothermometer is applied to a ferrosalite–eulite coexistence at Lac Huguette, it suggests a 750°C temperature as well; however, a salite–hypersthene pair from Mount Reed plots closer to their 850°C isotherm. The many analyses for pyroxene pairs by Kranck (1961) and Butler (1969) produced a very large scatter about Ross and Huebner's (1975) isotherms, undoubtedly because their chemical analyses were made on mineral separates, instead of by electron microprobe techniques *in situ*. Their pyroxene pairs, therefore, could not be used for temperature estimates.

Three further constraints in the assessment of the maximum temperatures and pressures attained in the highest metamorphic-grade area (Gagnon–Mount Reed–Lac des Silicates) are: (1) the great abundance of medium- to coarse-grained muscovite in qtz–musc–spec schists in the Gagnon region, (2) the sporadic occurrence of kyanite in the Gagnon region, and (3) the occurrence of orthoferrosilite in the nearby Mount Reed assemblages. The muscovite is euhedral, generally coarse-grained, and completely unaltered, indicating that the Gagnon region rocks attained temperatures within the muscovite stability field. As it has an average FeO content of approximately 6.5 weight percent (equivalent to 7.2 weight percent Fe_2O_3), its stability field is probably somewhat less extensive in P–T space than that of pure muscovite (Velde, 1965). The occurrence of kyanite in the Gagnon as well as Labrador City areas indicates that the rocks over a large geographic region recrystallized within the kyanite stability field as well. The presence of quite abundant orthoferrosilite–quartz in several Mount Reed assemblages allows for an independent minimum pressure estimate on the basis of the orthoferrosilite composition. The averaged Fe/(Ca+Fe+Mg+Mn) content of the most Fe-rich orthoferrosilite (see also Table 4) is 0.937. This composition can be related to the experimental work of Smith (1971) by a quantitative extrapolation procedure as outlined by Wood (1975). From this procedure the minimum pressure estimate for the Mount Reed orthofer–mag–qtz assemblage, in the absence of olivine, is 11–12 kbar. Bohlen *et al.* (1978) conclude, on the basis of new experimental work, that such estimates are about 1–2 kbar too high, which leads to a final estimate of the load pressure of about 10–11 kbar. Ormaasen's (1977) extrapolations lead to a very similar pressure estimate, and Jaffe *et al.* (1978) derive similar load pressures for an orthoferrosilite gneiss occurrence. Figure 5 outlines a possible region of metamorphic intensity for the Gagnon–Mount Reed region of about 700 to 750°C and 10–11 kbar load pressure. In short, the iron-formations of this study have undergone metamorphic changes from the late diagenetic stage at about 150°C and 1–2 kbar to the maximum metamorphic intensity shown in the

Gagnon region. A possible prograde temperature path is indicated in Figure 5. The Mount Reed–Gagnon–Lac des Silicates areas appear to represent the highest metamorphic temperatures, whereas the amphibole-rich assemblages in the Labrador City–Bloom Lake–Mount Wright area formed at a somewhat lower temperature, or higher water pressure, or both.

Acknowledgments

This study would not have been possible without the generous hospitality and field support of the two major iron mining companies in the southern extension of the Labrador Trough. The Iron Ore Company of Canada, in the summer of 1961, provided hydroplane and field camp support for study and sampling of most of the sample localities north of the Labrador City area. The Quebec Cartier Mining Company, during the summer of 1973, provided me access to the Mount Wright, Mount Reed, Gagnon, Lac Hugette, and Lac Moiré regions by various company aircraft. In the summer of 1975 the Quebec Cartier Company further allowed me to sample various exploration drill cores in their Port Cartier facilities. That same summer I did field and diamond drill core sampling in the D'Aigle Bay Region with the support of the Iron Ore Company of Canada. To the various staff geologists who aided me in the preparation for the field work I express my sincere thanks.

LaVerne M. Friberg and Michael R. Hudson are thanked for their aid in obtaining part of the electron microprobe data. Peter A. Moreau and Mrs. Chris Hudson aided in the data processing for the computer-generated triangular diagrams. I thank Maynard Coller for some of the bulk chemical analyses, Messrs. W. H. Moran, R. T. Hill, and G. R. Ringer for drafting and photography, and Mrs. Charles L. Brown for the typing of the manuscript. I am grateful to Harold L. James, Charles V. Guidotti and C. Stephen Haase for their constructive reviews of this paper.

Field and laboratory support for this study were provided by NSF grants GA-11435, GA-36186, and EAR-76-11740 (Klein). The electron microprobe used in this study was obtained by joint funding from NSF grant GA-37109 and the Indiana University Foundation.

References

Bohlen, S. R., A. L. Boettcher and E. J. Essene (1978) Experimental reinvestigation of ferrosilite–fayalite–quartz stability (abstr.). *Trans. Am. Geophys. Union, EOS, 58*, 402.

Bonnichsen, B. (1969) Metamorphic pyroxenes and amphiboles in the Biwabik Iron Formation, Dunka River area, Minnesota. *Mineral. Soc. Am. Spec. Pap., 2*, 217–239.

Butler, P., Jr. (1969) Mineral compositions and equilibria in the metamorphosed iron-formation of the Gagnon region, Quebec, Canada. *J. Petrol., 10*, 56–101.

Chatterjee, N. D. and W. Johannes (1974) Thermal stability and standard thermodynamic properties of synthetic $2M_1$ muscovite, $KAl_2[AlSi_3O_{10}(OH)_2]$. *Contrib. Mineral. Petrol., 48*, 89–114.

Dahl, P. S. (1977) *The mineralogy and petrology of Precambrian metamorphic rocks from the Ruby Mountains, southwestern Montana.* Ph.D. Thesis, Indiana University, Bloomington, Indiana.

Fahrig, W. F. (1967) Shabogamo Lake map-area, Newfoundland–Labrador and Quebec. *Geol. Surv. Can. Mem. 354.*

Ferry, J. M. (1976) P, T, f_{CO_2}, and f_{H_2O} during metamorphism of calcareous sediments in the Waterville–Vassalboro area, south-central Maine. *Contrib. Mineral. Petrol., 57*, 119–143.

——— (1977) A study of isobaric, isothermal metamorphism of argillaceous carbonate rocks: implications for fluid flow. *Carnegie Inst. Wash. Year Book, 76*, 607–613.

Floran, R. J. and J. J. Papike (1975) Petrology of the low-grade rocks of the Gunflint Iron Formation, Ontario–Minnesota. *Bull. Geol. Soc. Am., 86*, 1169–1190.

——— and ——— (1978) Mineralogy and petrology of the Gunflint Iron Formation, Minnesota–Ontario: correlation of compositional and assemblage variations at low to moderate grade. *J. Petrol.*, in press.

French, B. M. (1968) Progressive contact metamorphism of the Biwabik Iron Formation, Mesabi Range, Minnesota. *Minnesota Geol. Surv. Bull. 45.*

——— (1973) Mineral assemblages in diagenetic and low-grade metamorphic iron-formation. *Econ. Geol., 68*, 1063–1075.

Gair, J. E. (1975) Bedrock geology and ore deposits of the Palmer Quadrangle, Marquette County, Michigan. *U.S. Geol. Surv. Prof. Pap. 769.*

Gross, G. A. (1968) Geology of iron deposits in Canada, vol. 3, Iron Ranges of the Labrador Geosyncline. *Geol. Surv. Can. Econ. Geol. Rep. 22.*

Hey, M. H. (1954) A new review of the chlorites. *Mineral. Mag., 30*, 277–292.

Holdaway, M. J. (1971) Stability of andalusite and the aluminum silicate phase diagram. *Am. J. Sci., 271*, 97–131.

Immega, I. P. and C. Klein (1976) Mineralogy and petrology of some metamorphic Precambrian iron-formations in southwestern Montana. *Am. Mineral., 61*, 1117–1144.

Jaffe, H. W., P. Robinson and R. J. Tracy (1978) Orthoferrosilite and other iron-rich pyroxenes in microperthite gneiss of the Mt. Marcy area, Adirondack Mountains. *Am. Mineral., 63*, in press.

James, H. L. (1954) Sedimentary facies of iron-formation. *Econ. Geol., 49*, 235–293.

——— (1955) Zones of regional metamorphism in the Precambrian of northern Michigan. *Bull. Geol. Soc. Am., 66*, 1455–1488.

Klein, C. (1966) Mineralogy and petrology of the metamorphosed Wabush Iron Formation, southwestern Labrador. *J. Petrol., 7*, 246–305.

——— (1968) Coexisting amphiboles. *J. Petrol., 9*, 281–330.

——— (1973) Changes in mineral assemblages with metamorphism of some banded Precambrian iron-formations. *Econ. Geol., 68*, 1075–1088.

——— (1974) Greenalite, stilpnomelane, minnesotaite, crocidolite, and carbonates in a very low-grade metamorphic iron-formation. *Can. Mineral., 12*, 475–498.

——— and R. P. Fink (1976) Petrology of the Sokoman Iron Formation in the Howells River area, at the western edge of the Labrador Trough. *Econ. Geol., 71*, 453–487.

——— and O. P. Bricker (1977) Some aspects of the sedimentary and diagenetic environment of Proterozoic banded iron-formation. *Econ. Geol., 72*, 1457–1470.

Kranck, S. H. (1961) A study of phase equilibria in a metamorphic iron-formation. *J. Petrol., 2*, 137–184.

Lesher, C. M. (1976) *Mineralogy and petrology of the Sokoman Iron Formation near Ardua Lake, Quebec.* M. A. Thesis, Indiana University, Bloomington, Indiana.

Mueller, R. F. (1960) Compositional characteristics and equilibrium relations in mineral assemblages of a metamorphosed iron formation. *Am. J. Sci., 258*, 449–497.

Ormaasen, D. E. (1977) Petrology of the Hopen mangerite–

charnockite intrusion, Lofoten, north Norway. *Lithos, 10,* 291–310.

Ross, M. and J. S. Huebner (1975) A pyroxene geothermometer based on composition–temperature relationships of naturally occurring orthopyroxene, pigeonite, and augite (abstr.). Abstracts, International Conference on Geothermometry and Geobarometry, The Pennsylvania State University.

Simmons, E. C., D. H. Lindsley and J. J. Papike (1974) Phase relations and crystallization sequence in a contact-metamorphosed rock from the Gunflint Iron Formation, Minnesota. *J. Petrol., 15,* 539–565.

Smith, D. (1971) Stability of the assemblage iron-rich orthopyroxene–olivine–quartz. *Am. J. Sci., 271,* 370–382.

Velde, B. (1965) Phengite micas: synthesis, stability, and natural occurrence. *Am. J. Sci., 263,* 886–913.

Wood, B. J. (1975) The application of thermodynamics to some subsolidus equilibria involving solid solutions. *Fortschr. Mineral.,* special issue to vol. 52, 21–45.

Zajac, I. S. (1974) The stratigraphy and mineralogy of the Sokoman Formation in the Knob Lake area, Quebec and Newfoundland. *Geol. Surv. Can. Bull. 220.*

Manuscript received, March 27, 1978; accepted for publication, May 19, 1978.